ChemPubSoc Europe

DOI: 10.1002/cctc.201900333

CHEMCATCHEM Full Papers

Characterization of Type IV Carboxylate Reductases (CARs) for Whole Cell-Mediated Preparation of 3-Hydroxytyrosol

Melissa Horvat,[a] Susanne Fritsche,[a] Robert Kourist,[b] and Margit Winkler*[a, b]

Fragrance and flavor industries could not imagine business without aldehydes. Processes for their commercial production raise environmental and ecological concerns. The chemical reduction of organic acids to aldehydes is challenging. To fulfill the demand of a mild and selective reduction of carboxylic acids to aldehydes, carboxylic acid reductases (CARs) are gaining importance. We identified two new subtype IV fungal CARs from *Dichomitus squalens* CAR (*Ds*CAR) and *Trametes versicolor* CAR (*Tv2*CAR) in addition to literature known *Trametes versicolor* CAR *(Tv*CAR*)*. Expression levels were improved by the co-expression of GroEL-GroES with either the trigger factor or the DnaJ-DnaK-GrpE system. Investigation of the substrate scope of the three enzymes revealed overlapping substrate-specificities. *Tv2*CAR and *Ds*CAR showed a preferred pH range of 7.0 to 8.0 in bicine buffer. *Tv*CAR showed highest activity at pH 6.5 to 7.5 in MES buffer and slightly reduced activity at pH 6.0 or 8.0. *Tv*CAR appeared to tolerate a wider pH range without significant loss of activity. Type IV fungal CARs optimal temperature was in the range of 25–35 °C. *Tv*CAR showed a melting temperature (T_m) of 55 °C indicating higher stability compared to type III and the other type IV fungal CARs (T_m 51–52 °C). Finally, *Tv*CAR was used as the key enzyme for the bioreduction of 3,4-dihydroxyphenylacetic acid to the antioxidant 3-hydroxytyrosol (3-HT) and gave 58 mM of 3-HT after 24 h, which correlates to a productivity of 0.37 g L^{-1} h^{-1}.

Introduction

Increasing sustainability of chemical processes is one of the key goals in industrial biotechnology today.[1] Chemical production turns away from generating hazardous substances and targets the utilization of renewable resources.[2,3] Within the last decades, the developments achieved in biological techniques and tools have enabled the engineering of microorganisms for catalytic conversions.[4] Through inexpensive, renewable substrates and high cell density fermentation processes, biotechnology is more widely introduced in industry.[5] Carboxylic acid reductases (CARs, E.C. 1.2.1.30) are the enzymes of choice to reduce carboxylic acids to aldehydes. Their 3-domain-architecture as well as the reaction scheme are displayed in Figure 1. Their ATP and NADPH dependent mechanism was affirmed by the determination of protein crystal structures of separate adenylation and reductase domains of bacterial CARs and modelling.[6] CARs are frequently introduced into cascade reactions *in vivo*. In many cases, endogenous enzymes such as aldehyde reductases, decarbonylases and alcohol dehydrogenases within the expression hosts are being utilized e.g. to reduce the aldehyde to the corresponding alcohol,[7–9] and CARs may become the limiting step in such reaction sequences.[10] To create more variety for cascade applications, a repertoire of characterized key enzymes is of most importance.

Within recent years, various bacterial and few fungal CARs have been described in literature. A detailed list can be found in SI Table S1. A phylogenetic analysis revealed that all 30 experimentally confirmed bacterial CARs are categorized as subtype I and seemed to be relatively conserved, whereas the 4 fungal CARs with very low sequence identities (< 25 %) fall into three distinct subclasses.[11,12] The activity of fungal CAR from the ascomycete *Neurospora crassa* was described in 1968 by Gross *et al.*[13] In 2016, the gene sequence was associated to the protein and cloned into *E. coli* with an additional phosphopantetheinyl transferase from *E. coli*.[14] Like other CARs,[15] *Neurospora crassa* CAR (*Nc*CAR) requires the co-expression of a phosphopantetheinyl transferase. Biophysical characterization of the type III *Nc*CAR enzyme indicated a preference for an acidic environment (pH 5.5–6.0) and a broad substrate tolerance.[14,16] *Aspergillus terreus* CAR (*At*CAR)[17] and *Stachybotrys bisbyi* CAR (*Sb*CAR)[18] belong to the subtype II and are the only CARs so far placed in this same subtype.[12] The first and only CAR of subtype IV was described from *Trametes versicolor* (*Tv*CAR) and was functionally expressed in rather low amounts. Partially purified enzyme preparations of the *Tv*CAR were used to explore its substrate scope. Surprisingly, it showed similar specific activities for aromatic, aliphatic and substituted aromatic carboxylic acids.[19] For the reduction of aliphatic substrates the bacterial *Mm*CAR from *Mycobacterium marinum* was utilized almost exclusively so far.[8]

[a] M. Horvat, S. Fritsche, Priv.-Doz. M. Winkler
acib – Austrian Center of Industrial Biotechnology
Petersgasse 14, 8010 Graz (Austria)
E-mail: margitwinkler@tacib.at
[b] Prof. R. Kourist, Priv.-Doz. M. Winkler
Institute of Molecular Biotechnology
Graz University of Technology
Petersgasse 14, 8010 Graz (Austria)

Supporting information for this article is available on the WWW under https://doi.org/10.1002/cctc.201900333

This manuscript is part of the Special Issue dedicated to the Women of Catalysis.

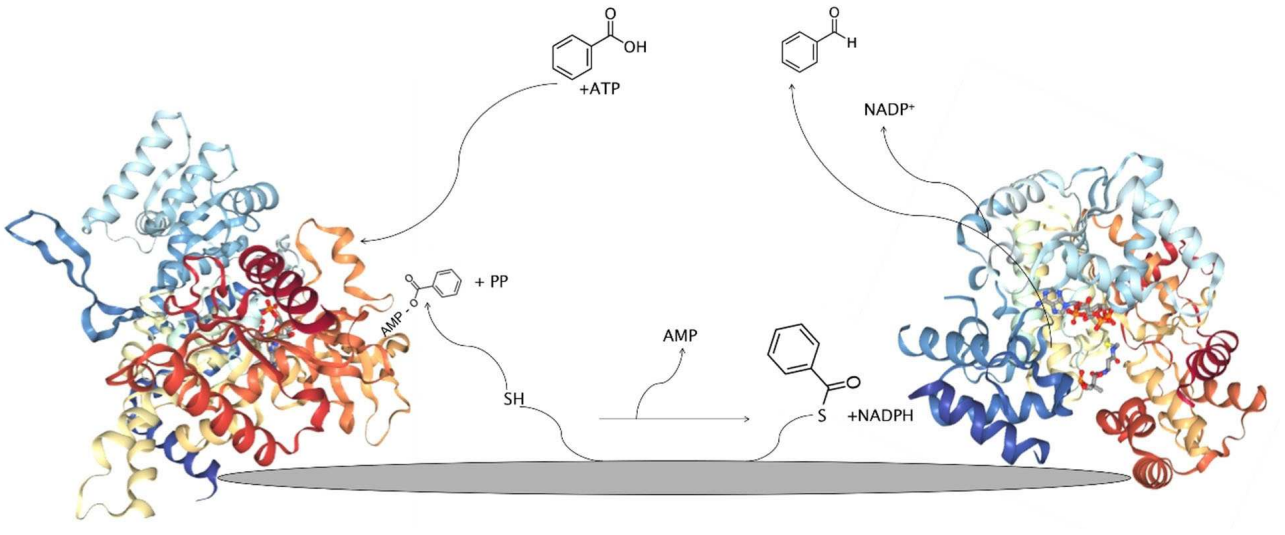

Figure 1. Schematic reaction mechanism of CAR enzymes (E.C. 1.2.1.30). Left: ATP and substrate enter the active site of the adenylation domain. The structure of the adenylation domain of *Nocardia iowensis* CAR (*Ni*CAR) is shown in complex with AMP (PDB ID: 5MSC).[6] The substrate is then activated as an AMP anhydride and pyrophosphate is released.[3] Middle: A thioester is formed at the phosphopantetheine binding site (grey), and AMP is released. Right: the thioester is translocated to the reductase domain (PDB ID: 5MSO).[6] The reductase domain in the scheme is from *Mycobacterium marinum* in complex with $NADP^+$. The last step is thioester reduction and release of the aldehyde and $NADP^+$. Microsoft Power Point and ChemDraw were used to generate the figure.

To broaden our understanding of CARs within one phylogenetic category, one goal is to improve expression of *Tv*CAR and to explore its characteristics and limitations in more depth. The second goal is to uncover further fungal CARs.

In this study, we explored the hidden potential of fungal CARs to increase the number of biocatalytic tools for reducing carboxylic acids and broaden the operational space for potential industrial applications. We identified two new type IV fungal CARs and described their phylogenetic relations to the family of CARs. Two CARs from *Trametes versicolor* and one from *Dichomitus squalens* were heterologously expressed in *E. coli*. Low expression levels increased by co-expressing chaperone systems GroEL-GroES with either the trigger factor or the DnaJ-DnaK-GrpE system to enhance the affinity for proteins to promote their folding. To determine substrate specificities of type IV CARs, specific activities towards a range of aliphatic and aromatic substrates have been determined. We investigated the effects of pH and temperature and finally the reduction of the model substrate 3,4-dihydroxyphenylacetic acid (DOPAC) to 3-hydroxytyrosol (3-HT). We improved the reduction of DOPAC to 3-HT, a highly potent antioxidant with various applications in cosmetics and food supplements. The preparation of 3-HT from DOPAC has the potential to attain a 45-fold value increase by pursuing the biosynthetic route. We achieved a production of 0.37 $g L^{-1} h^{-1}$ for 3-HT (2.4 $mM h^{-1}$) that after further optimization may lead to an alternative method for producing 3-HT.

Results and Discussion

Alignment and Phylogenetic Analysis

Up to date, 30 functional CARs have been described (list of CARs with references see SI Table S1). Among these, only five CARs do not originate from bacteria. These few CARs constitute three of four phylogenetic types of CARs.[14,18–20] Further representatives of fungal CARs are not only needed to diversify the basis of phylogenetic analyses and corroborate conclusions from such analyses, but also to eventually assemble a repertoire of new enzymes with different characteristics. The protein sequences of *Ni*CAR,[21,22] *Mm*CAR,[8] *Sro*CAR[23] and *At*CAR[17,20] were taken as templates for a BLASTp search with the restriction to organisms with experimentally confirmed ability to reduce carboxylic acids. Hit sequences were further analyzed for the presence of essential key residues and motifs.[16,24] Putative CAR sequences from *Dichomitus squalens* (*Ds*CAR) and *Trametes versicolor* (*Tv2*CAR) were top rated. Both CAR candidates were chosen for further characterization, as phylogenetic analysis revealed that *Ds*CAR and *Tv2*CAR were both type IV CARs, for which *Tv*CAR is the only experimentally confirmed CAR so far[19] (Figure 2). Sequence analyses (SI Figure S1) of the CARs displayed in the phylogenetic tree (Figure 2) revealed that type IV CAR sequences of *Trametes versicolor* were 65.1% identical, whereas the *Ds*CAR showed 39.6% sequence identity to *Tv*CAR and 39.8% to *Tv2*CAR, respectively.

Expression and Purification

New CARs were cloned and expressed from the pETDuet-1 plasmid in *E. coli* MG1655 RARE (DE3) as previously established

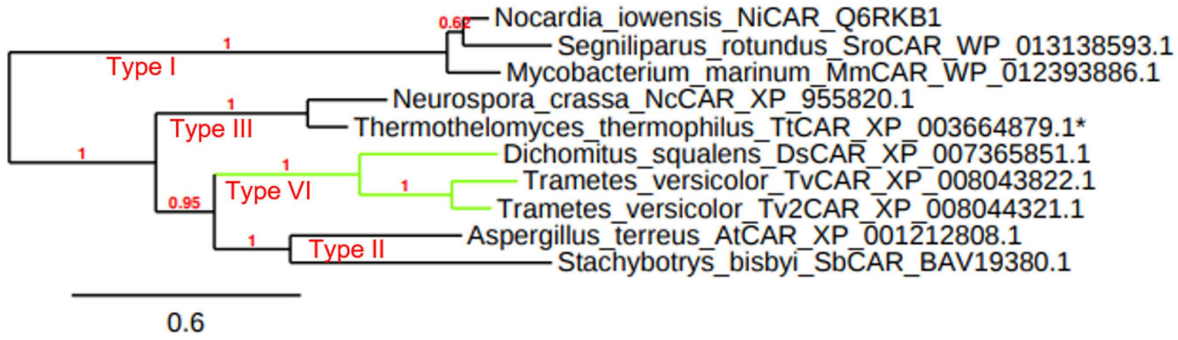

Figure 2. A phylogenetic tree of fungal and bacterial CAR enzymes, categorized in four subtypes. Newly discovered sequences and previously described CARs[8,14,15,18,19,23] were incorporated in the phylogenetic analysis. Green branches represent CARs investigated in this study. **Tt*CAR was identified in *Thermothelomyces thermophilus*, which is also known as *Myceliophthora thermophila, Thielavia heterothallica ATCC 42464,* or *Sporiotrichum thermophile.*

in our lab.[12,14] This strain harbors specific knock outs that reduce its ability to reduce aromatic aldehydes further to their corresponding alcohols.[25] *Ds*CAR was well expressed, whereby approximately equal amounts were detected in soluble and insoluble fraction (Table 1 and SI Figure S4A). This indicated a steady translation and protein folding of *Ds*CAR.[26,27]

Table 1. CARs in this study.

Abbreviation	Organism	NCBI Reference	Calculated size [kDa]	Ratio soluble/ insoluble fraction
*Tv*CAR	*Trametes versicolor*	XP_008043822.1	118.2	0.341
*Tv2*CAR	*Trametes versicolor*	XP_008044321.1	118.6	0.178
*Ds*CAR	*Dichomitus squalens*	XP_007365851.1	121.2	1.059

[a] The size of the CAR enzymes was calculated via ExPASy. [b] Protein bands were quantified via G:Box HR16 by Syngene.

Determination of the total protein concentration of *Ds*CAR resulted in ~14 mg per 400 mL of cultivation [~4.2 g cell wet weight (CWW)]. *Tv*CAR showed an expression of ~10 mg protein in the soluble fraction per 400 mL cultivation, (~4.1 g CWW). *Tv2*CAR was expressed the weakest. Most protein was found in the insoluble fraction. The amount of CAR was less than ~5 mg per 400 mL of cultivation (~4.1 g CWW). According to Sorensen and Morensen, the following strategies for improving the solubility of proteins without engineering the target was suggested: to investigate various temperatures, strains, media, molecular chaperones or include tRNA complementation plasmids.[26] An optimized expression medium and autoinduction protocol at 20 °C (SI Figure S4) as described by Studier showed the best results for CARs in our previous studies and was used as our expression standard.[28]

Improvement of CAR Expression Levels

Whole cell-mediated conversions are dependent on the amount of functional enzyme, cell wall transport and substrate acceptance, among other factors (SI Table S4).[29,30] *In vitro* bioreductions catalyzed by *Tv*CAR showed that only the soluble protein fraction was functional and responsible for reductase activity (SI Figure S5). Hence, an increase in soluble protein should increase the specific catalyst activity. Therefore, *E. coli* strains which were known to be beneficial for protein expression, translation and folding[31,32] were transformed with plasmid pETDuet-1:*Ec*PPTase:*Tv2*CAR (Table 2). This construct encodes the CAR with the weakest expression level *Tv2*CAR (SI Figure S4).

E. coli strains were transformed with pETDuet-1:*EcPPTase* or the empty pETDuet-1 vector, respectively. Both served as negative controls. After cultivation and induction at standard conditions, 50 OD units of each strain were analyzed by conducting whole cell-mediated reduction of piperonylic acid **1a** to show the impact of the expression level on catalyst efficiency. In parallel, another 50 OD units of each cultivation were used to determine the levels of soluble and insoluble expression. All *E. coli* BL21 (DE3) TaKaRa [pG-KEJ8]/[pG-Tf2]/[pGro7]/[pTF16] strains showed improved soluble expression levels compared to the expression level of *Tv2*CAR without co-expression of chaperones (see Table 2 and SI Figure S4).

Due to the highest conversions and best soluble expression levels of *Tv2*CAR, the plasmids [pG-KEJ8] and [pG-Tf2] were chosen for further experiments with *Tv*CAR in *E. coli* MG1655 RARE (DE3). This specific *E. coli* strain was engineered to maintain aromatic aldehydes and minimize their reduction to alcohols by knocking-out genes encoding for aldo-ketoreductases and alcohol dehydrogenases.[25] Chaperones GroEL-GroES with additional helper proteins such as the triggering factor (TF) or the DnaK-DnaJ-GrpE system positively influenced the folding behavior of *Tv2*CAR and *Tv*CAR (Figure 3B). The increased level of soluble proteins found in the cell translated to increased activity (Figure 3A). An increase of up to ~40% in conversion was achieved when *Tv2*CAR was co-expressed with GroEL-GroES and DnaK-DnaJ-GrpE system (Figure 3A). Similar improvements of soluble expression were achieved with the

Table 2. Ratios of soluble to insoluble protein fractions of *Tv2*CAR with co-expressed chaperones or expressed in optimized expression hosts and catalyst efficiency determined by whole cell biotransformations [%].

Expression system of *Tv2*CAR[a]	*E. coli* strain/plasmid feature	Ratio soluble/insoluble protein fraction[b]	Absolute amounts of soluble protein [mg][c]	Conversion [%][d]
*Tv2*CAR in *E. coli* K-12 MG1655 RARE (DE3)	Engineered for reduced reduction of aromatic aldehydes	0.178	4.7	25.8 ± 7.0
*Tv2*CAR [pGro7] in *E. coli* BL21 (DE3)	Co-expression GroES-GroEL	0.327	8.7	38.9 ± 3.9
*Tv2*CAR [pKJE7] in *E. coli* BL21 (DE3)	Co-expression DnaK-DnaJ-GrpE	0.221	5.8	43.2 ± 3.9
*Tv2*CAR [pG-KJE8] in *E. coli* BL21 (DE3)	Co-expression GroES-GroEL-DnaK-DnaJ-GrpE	0.385	10.2	63.3 ± 4.7
*Tv2*CAR [pTF16] in *E. coli* BL21 (DE3)	Co-expression of trigger factor (Tf)	0.297	7.9	19.4 ± 4.7
*Tv2*CAR [pG-TF2] in *E. coli* BL21 (DE3)	Co-expression of GroES-GroEL-Tf	0.393	10.4	59.0 ± 3.3
*Tv2*CAR in *E. coli* BL21 CodonPlus (DE3)-RP	Contain extra copies of the *argU* and *proL* genes for increasing tRNA pool	N/A	N/A	19.6 ± 4.7
*Tv2*CAR in *E. coli* Origami B (DE3)	Mutations in *lacZY, trxB* and *gor* for enhancing disulfide bonds	N/A	N/A	14.9 ± 0.7
*Tv2*CAR in *E. coli* Rosetta-gami (DE3)	Combine codon bias and enhance disulfide bond formation	N/A	N/A	11.8 ± 0.4
*Tv2*CAR in *E. coli* Tuner (DE3)	lac permease (lacY) mutation for controlled induction	N/A	N/A	25.9 ± 4.7

[a] Chaperone plasmid set was commercially available at TaKaRa BIO Inc (catalogue number 3340). [b] Protein bands were quantified via G:Box HR16 by Syngene. N/A: not applicable, bands too faint for evaluation. [c] Absolute amounts of soluble protein was estimated based on 400 mL shake flask cultivation of *E. coli* K12 MG1655 RARE (DE3) [pETDuet-1:*Ec*PPtase:*Tv2*CAR] followed by a Ni-affinity chromatography purification of *Tv2*CAR. [d] Whole cell-mediated reductions of piperonylic acid were performed in triplicates.

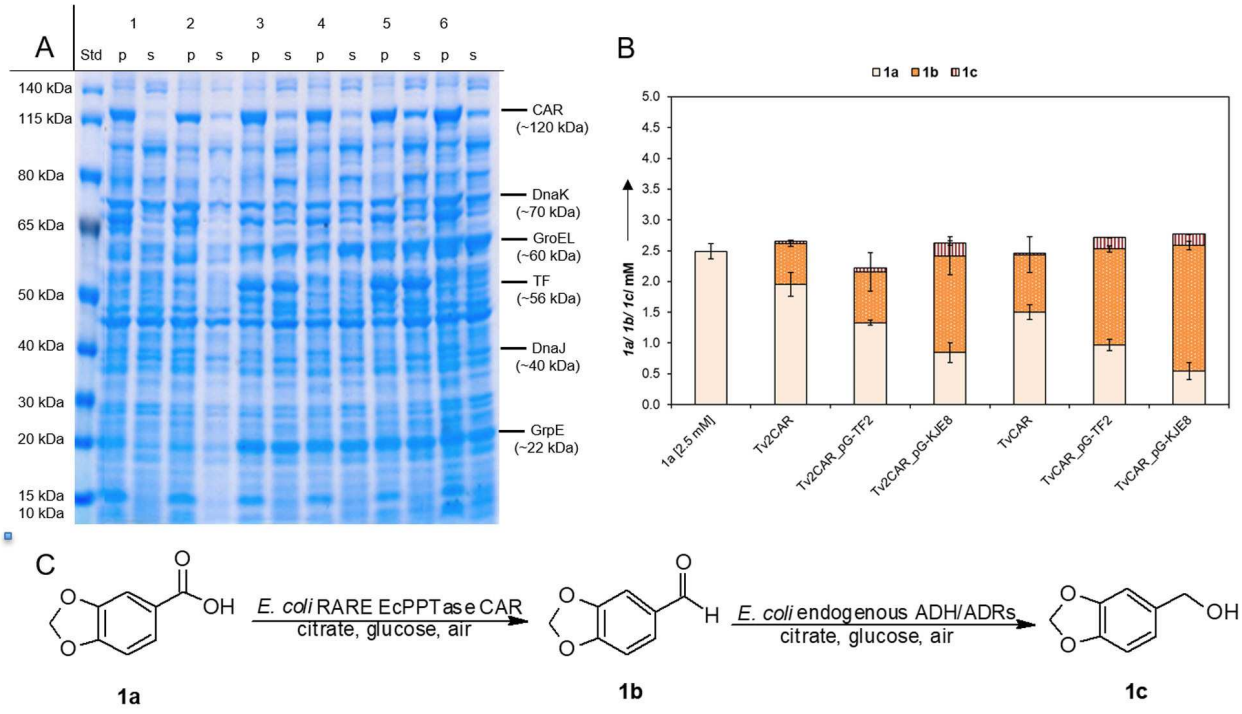

Figure 3. A) Expression analysis of *Tv2*CAR and *Tv*CAR, co-expressed with chaperones. Lane 1p-s: insoluble (p) and soluble (s) fraction of *Tv2*CAR. Lane 2 p–s: insoluble (p) and soluble (s) fraction of *Tv*CAR. Lane 3p-s: insoluble (p) and soluble (s) fraction of *Tv2*CAR with [pG-TF2]. Lane 4p–s: insoluble (p) and soluble (s) fraction of *Tv2*CAR with [pG-KEJ8]. Lane 5p–s: insoluble (p) and soluble (s) fraction of *Tv*CAR with [pG-TF2]. Lane 6p–s: insoluble (p) and soluble (s) fraction of *Tv*CAR with [pG-KEJ8]. SDS 4–12% Bis-Tris-gel. 60 min at 200 V in MOPS-buffer; staining: Simply Blue™ solution, ladder: PageRuler™ Prestained Protein Ladder (10–140 kDa). B) Whole cell-mediated reduction of **1 a** by *Tv2*CAR (~120 kDa) or *Tv*CAR (~120 kDa) expressed in *E. coli* K-12 MG1655 RARE (DE3) [pETDuet-1:*Ec*PPTase:*Xy*CAR] with or without chosen co-expression of chaperones GroEL (~60 kDa)-GroES (~22 kDa) and trigger factor (~56 kDa) [pG-TF2] or GroEL-GroES with DnaK (~70 kDa)-DnaJ (~40 kDa)-GrpE (~22 kDa) [pG-KEJ8]. Beige: **1 a**; orange: **1 b**; red striped: **1 c**. Error bars show the standard deviation of three sets of technical triplicates. C) Reaction scheme of whole cell-mediated reduction of **1 a** by CAR.

Table 3. Specific activities[a] of CARs for various aromatic and aliphatic substrates determined by monitoring NADPH depletion. Chemical structures of substrates are displayed in the supporting information Figure S3.

Substrate[b]	*Tv*CAR [U mg^{-1}]	*Tv2*CAR [U mg^{-1}]	*Ds*CAR [U mg^{-1}]
Aromatic substrates			
Piperonylic acid (**1 a**)	0.79 ± 0.05	0.87 ± 0.08	0.46 ± 0.01
Benzoic acid (**2 a**)	0.35 ± 0.02	0.78 ± 0.03	0.82 ± 0.06
DOPAC (**3 a**)	0.43 ± 0.00	0.30 ± 0.01	0.50 ± 0.02
Aliphatic substrates			
Pentanoic acid (**4 a**)	0.65 ± 0.03	0.22 ± 0.02	0.47 ± 0.02
Hexanoic acid (**5 a**)	0.40 ± 0.10	0.45 ± 0.03	0.24 ± 0.01
Heptanoic acid (**6 a**)	0.41 ± 0.03	0.34 ± 0.02	0.26 ± 0.02
Octanoic acid (**7 a**)	0.24 ± 0.00	0.14 ± 0.02	0.21 ± 0.01
Nonanoic acid (**8 a**)	0.31 ± 0.07	0.30 ± 0.03	0.05 ± 0.01
Decanoic acid (**9 a**)	0.31 ± 0.02	0.30 ± 0.09	0.03 ± 0.03

[a] One activity unit is defined as the amount of enzyme preparation catalyzing the oxidation of 1 μM of NADPH per minute. [b] Standard deviations were calculated on basis of four measurements. Blank reactions were conducted with no ATP.

co-expression of GroEL-GroES with TF. TF was described to bind to GroEL and increase its affinity for proteins to promote their folding.[33] The overexpression of TF showed similar effects to the overexpression of the DnaK-DnaJ-GrpE chaperone team in preventing aggregation of *Tv2*/*Tv*CAR, which is due to the highly similar function of DnaK and TF in folding nascent polypeptides.[31]

Determination of Substrate Scope

*Tv*CAR and *Tv2*CAR showed highly similar specific activities for fatty acids ranging from C5–C10, which is most likely due to high sequence similarity (~65.3 %). In addition to medium-chain aliphatic substrates tested previously,[19] *Tv*CAR reduces short chain aliphatic acids. The comparison of the initial rate activities for the reduction of acids over a period of ten minutes indicated benzoic acid **2 a** to be the preferred substrate of *Tv2*CAR and *Ds*CAR (Table 3). *Tv2*CAR and *Ds*CAR showed higher activity for aromatic acids than for the aliphatic carboxylic acids. *Ds*CAR seemed to be significantly less efficient for fatty acid reduction than the CARs from *T. versicolor*. All CARs were tolerant to all tested substrates, with a clear preference towards aromatic and shorter aliphatic acids. Interestingly, *Tv*CAR showed lower specific activity for benzoic acid as compared to aliphatic substrates. This supports the hypothesis that each organism might have multiple CARs for reducing different substrates.[19]

Biochemical Characterization of CARs

Enzymes evolved to perform their function in specific cellular environments. Therefore, they should be adapted to the biophysical characteristics, e.g. pH and temperature, of their respective cellular compartment. Many enzyme properties, such as activity and stability, are pH dependent.[34]

Effect of Reaction pH

For determination of the optimal pH environment for the fungal type IV CARs their activity at different pH and buffer systems was assessed. Correlating with their preferred substrate, an aliphatic substrate (**7 a**) was used for the pH assessment of *Tv*CAR and an aromatic substrate (**2 a**) for *Tv2*CAR and *Ds*CAR. The relative activity analysis of *Tv*CAR revealed a preferred neutral to acidic environment. The optimum pH for *Tv*CAR was identified as pH 7.0 in 100 mM MES-NaOH. Overall, *Tv*CAR showed activity in a rather broad range from pH 6.0-8.0 without losing activity considerably (Figure 4A). This observation was consistent with the biophysical characterizations of other CARs.[10,24] The pH optimum determined for *Tv2*CAR and *Ds*CAR showed the highest relative activity at pH 7.5 in 100 mM bicine-NaOH buffer and showed a preference for neutral to basic aqueous environment (Figure 4B–C).

Commonly used buffer constituents are acetate or citrate. Being carboxylic acids, they may partly be reduced by CARs. However, CAR activity for citric acid was below detection limit under these conditions. The inhibition effect of potassium phosphate buffer is most likely due to binding of phosphate at the ATP-binding site in the adenylation domain.

Effect of Temperature

Activity and stability are important characteristics when it comes to temperature dependent properties of enzymes.[34] From a biocatalytic point of view, high activity is important while stability can be enhanced in most cases by additives e.g. DTT, NaCl, etc. and protein engineering. To investigate the stability of type IV fungal CARs, the midpoint temperatures of protein unfolding transitions (T_m) and the temperature optimum of *Tv*CAR, *Tv2*CAR and *Ds*CAR were determined.

To determine thermostabilities of type IV fungal CARs, thermal shift assays were performed in different buffer systems and a pH range from 4.6–9.0.[35] *Tv*CAR showed a T_m of 55 °C in potassium phosphate buffer at pH 6.5 (Table 4). The addition of

0.1 M NaCl increased the unfolding temperature by 1 °C (SI Figure S6). Using the thermal shift assay for type III CAR from *Neurospora crassa* (*Nc*CAR), the T_m was 51 °C in potassium phosphate buffer with 0.1 M NaCl, pH 7.0 (Table 4) whereas *Tv2*CAR and *Ds*CAR showed a T_m of 52 °C in potassium phosphate buffer at pH 7.5. Notably, the reported T_m of *Nc*CAR at 45 °C was determined by NanoDSF.[14] For storage of *Tv*CAR, and CARs in general, phosphate buffer showed stabilizing effects, which is most likely explained by the binding of phosphate in the adenylation domain. Comparison of the most thermostable type IV fungal *Tv*CAR with the type III *Nc*CAR (SI Figure S6A and B) suggests that *Tv*CAR is slightly more thermostable under a wider range of pH than *Nc*CAR, which only showed a peak above 50 °C, when incubated in phosphate buffer.

To determine the optimal operational temperature for *in vitro* reactions, purified CAR preparations were used for NADPH-depletion analysis at temperatures varying from 25 °C–45 °C. Triplicate reactions proceeded for 1 h and relative activities were determined after workup. Previous studies of CAR enzymes were typically performed at 28 °C.[14–16,24] Our results (Figure 5) confirmed the reported temperature optima, as type IV fungal CARs showed 100% activity from 25 °C to 35 °C. For resting cells conversions utilizing *E. coli* cells, 37 °C may be of interest to facilitate co-factor recycling. However, CARs seemed to become slightly less active at 35 °C and above.

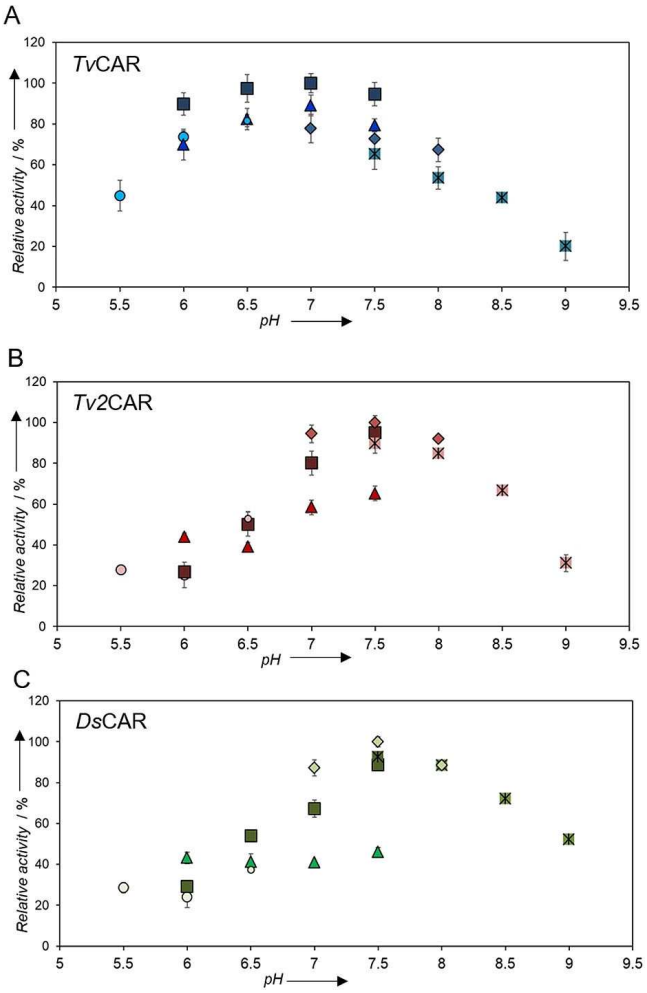

Figure 4. Relative activities of type IV fungal CARs in response to different pH values. Overlapping buffers containing 10 mM $MgCl_2$ were used to cover the pH range of 5.5–9.0. **7 a** (*Tv*CAR) and **2 a** (*Tv2*CAR and *Ds*CAR) was used as substrates and the activity relative to the highest activity at 100% is presented. **A)** *Tv*CAR. **B)** *Tv2*CAR. **C)** *Ds*CAR. ○: sodium citrate buffer, Δ: potassium phosphate buffer, □: MES-NaOH buffer, ◇: bicine-NaOH buffer, x: Tris-HCl buffer. Error bars show the standard deviation of three technical triplicates.

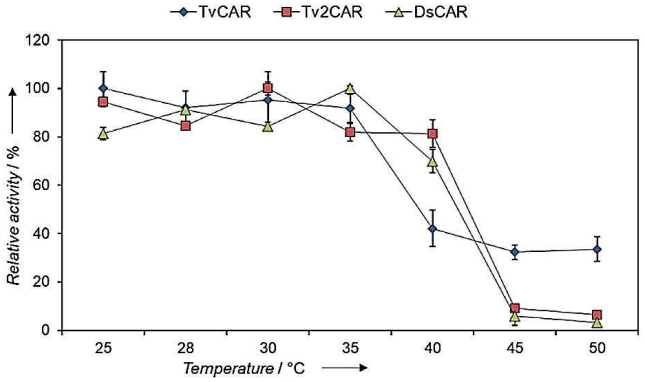

Figure 5. Relative activity of partially purified type IV fungal CARs in response to temperatures from 25–50 °C. Samples were incubated for 1 h and activity was indirectly determined through NADPH-consumption. **2 a** was used as substrate and the activity relative to the highest activity at 100% is presented. Error bars show the standard deviation of three technical triplicates. Blue diamonds: *Tv*CAR. Red squares: *Tv2*CAR. Green triangles: *Ds*CAR.

Table 4. Thermostability assessment of *Tv*CAR, *Tv2*CAR, *Ds*CAR and *Nc*CAR.[a]

Reaction buffer[b]	*Nc*CAR [T_m]	*Tv*CAR [T_m]	*Tv2*CAR [T_m]	*Ds*CAR [T_m]
PP, pH 6.5	50.7 ± 0.7	55.3 ± 0.6	50.6 ± 0.5	49.0 ± 0.0
PP, pH 6.5, with 0.1 M NaCl	51.0 ± 0.6	55.0 ± 0.0	50.3 ± 0.5	51.0 ± 0.0
PP, pH 7.0,	51.5 ± 0.6	55.0 ± 0.0	52.0 ± 0.0	52.0 ± 0.0
PP, pH 7.0, with 0.1 M NaCl	51.0 ± 0.0	55.0 ± 0.0	51.0 ± 0.0	52.3 ± 0.5
PP, pH 7.5	51.0 ± 0.6	54.0 ± 0.0	52.0 ± 0.0	52.0 ± 0.0
PP, pH 7.5, with 0.1 M NaCl	50.3 ± 0.6	54.0 ± 0.0	52.0 ± 0.0	52.3 ± 0.5

[a] Midpoint temperatures of protein unfolding transitions (T_m) determined by thermal shift assay. Each reaction was performed in technical triplicates. [b] All reaction buffers contained 10 mM $MgCl_2$. Potassium phosphate buffer is abbreviated PP.

Therefore, whole cell-mediated conversions such as performed with piperonylic acid **1a** are preferably performed at 28 °C. 35% activity was observed at 50 °C for *Tv*CAR, which correlates to the results of the stability assays. However, *Tv2*CAR and *Ds*CAR lost almost all activity at 45 °C. In comparison to characterized fungal CARs, *Tv*CAR seemed to be slightly more active at higher temperatures.[14] This observation confirmed also the results of the thermal shift assays when compared with *Nc*CAR. Consequently, it can be concluded that type IV fungal CARs showed no significantly reduced activity up to 35 °C and *Tv*CAR even remained active up to 50 °C when incubated for 1 h at the specific temperatures. Up to date only the bacterial *Mav*CAR was described to be more thermostable and active at temperatures higher than 40 °C.[10] Hence, *Tv*CAR would be a good fungal candidate when increased thermostability is needed. The broad substrate scope of *Tv*CAR, its improved heterologous expression, the good specific activity of DOPAC **3a** (~0.43 U mg^{-1}) and the acceptance of acidic pH conditions made *Tv*CAR a promising candidate for the overreduction of DOPAC to 3-HT.

Isoelectric Point

The isoelectric point (pI) of *Tv*CAR was both calculated and determined to minimize pH induced protein aggregation during e.g. purification procedures. The calculated pI of *Tv*CAR was 5.84, determined with ExPASy: SIB bioinformatics tool (https://web.expasy.org/compute_pi/), and was compared with an experimentally determined pI (SI Figure S7). A range of 5.0–5.4 for the pI of *Tv*CAR was determined by isoelectric focusing.

Synthetic Application of *Tv*CAR for Bioreduction of DOPAC to 3-HT

*Tv*CAR readily reduced 3,4-dihydroxyphenylacetic acid (DOPAC, **3a**) (Table 3). We previously investigated the reduction of **3a** to the antioxidant 3-hydroxytyrosol (3-HT, **3c**) using a whole cell biocatalyst, because the antioxidant 3-HT was in the spotlight of numerous studies to uncover its beneficial effects on human health.[36] 3-HT is abundant in olives *(Olea europaea)* and olive oil, and the health-promoting Mediterranean diet is partly ascribed to this compound. Due to its anticarcinogenic, anti-inflammatory, antiapoptotic and neuroprotective activities, 3-HT is already used in foods and cosmetics.[29,37,38] The high cost of purified **3c**, however, limits its availability on the market and is the bottleneck for its use.[36] The first generation catalyst for **3c** preparation harbored bacterial type I CAR from *Nocardia iowensis* (*Ni*CAR) as the key enzyme. The PPTase was co-expressed from a second plasmid.[39] Due to the whole cell approach, necessary cofactors were recycled intracellularly. After extensive optimization of the whole cell biotransformation, finally 27.9 mM of **3c** could be converted in 21 h using 30 mM of **3a** at a rather high cell density of OD120.[40]

We opted for *E. coli* BL21 (DE3) as the expression host for *Tv*CAR and *Ec*PPTase expression via the pETDuet-1 vector in the presence of [pG-KEJ8], to create a second-generation catalyst for **3c** preparation. **3c** formation was monitored, using 50 OD units of *E. coli* BL21 (DE3) [pG-KEJ8] [pETDuet-1:*Ec*PPTase:*Tv*CAR]. This corresponds to 48 mg mL^{-1} of wet cells. With **3a** concentrations varying from 10 to 60 mM, overall up to 58.2 mM of **3c** were formed within 24 h. This corresponds to 0.37 g L^{-1} h^{-1} (Figure 6), in comparison to

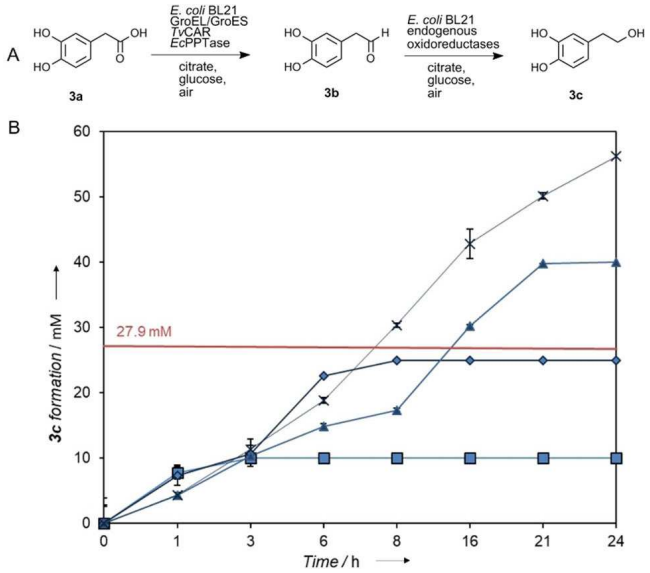

Figure 6. A–B) Scheme and whole cell-mediated biotransformation of **3a** to **3c** with 50 OD units of *E. coli* BL21 (DE3) [pG-KEJ8] [pETDuet-1:*Ec*PPTase:*Tv*CAR]. The 3-HT formation over different time points at 28 °C is depicted. Error bars show the standard deviation of three technical triplicates. The red line symbolizes the benchmark of 27.9 mM 3-HT previously achieved with 120 OD units over 21 h.[40] ■: 10 mM **3a** used as substrate. ▲: 25 mM **3a** used as substrate. ♦: 40 mM **3a** used as substrate. X: 60 mM **3a** used as substrate.

0.21 g L^{-1} h^{-1} using the first generation strain.[40] In 21 h, 49.4 mM of **3c** were detected when 60 mM of **3a** was used. By co-expressing chaperones to increase the amount of soluble CAR protein within the *E. coli* cells, using the validated pETDuet-1:*Ec*PPtase:*Tv*CAR expression set-up with the *Tv*CAR as well as using the *E. coli* BL21 (DE3) strain to facilitate high expression levels and the overreduction of 3,4-dihydroxyphey-lacetaldehyde **3b** to **3c**, a significant improvement of the synthesis of 3-HT (**3c**) was demonstrated. At the same time, the amount of cells was reduced from OD120 to OD50 which lead to a four-fold increase of biocatalyst yield (0.11 g/g versus 0.027 g/g based on cell wet weight, respectively) and a 1.7-fold improvement of the space-time-yield. A closed vessel set-up by using 15 mL glass tubes improved the mass balance. Previously, the mass balance was not satisfying due to the evaporation of the aqueous phase overnight in open reaction tubes. Summarizing, 3-HT formation was significantly more efficient using the second-generation biocatalyst with *Tv*CAR as the key enzyme for acid reduction.

Conclusions

New methods for the reduction of underivatized carboxylic acids are of high interest in view of sustainable chemistry that is needed for the valorization of renewable feedstock. Carboxylic acid reductases hold high potential in this respect. Uncovering more diversity in CARs from different phylogenetic subtypes is essential to build a useful toolbox for a broader substrate scope and extended operational space. We contributed to this field by extending the phylogenetic type IV fungal CARs with *Tv2*CAR and *Ds*CAR. Low expression levels of *Tv2*CAR and *Tv*CAR were improved by co-expressing chaperone systems GroEL-GroES and DnaK-DnaJ-GrpE or the TF. The increase of soluble protein correlated to the increase in activity when whole cell-mediated biotransformations were conducted. Investigation of specific activities from the same species (i.e. *Trametes versicolor*) suggested that species are using multiple CARs for different substrates. Hence, *Tv2*CAR demonstrated a tendency towards aromatic and *Tv*CAR towards aliphatic substrates. *Tv*CAR showed a pH optimum at pH 6.5–7.5 whereas *Tv2*CAR and *Ds*CAR seemed to prefer a pH of pH 7.0–8.0. Type IV fungal CARs optimal activity *in vitro* was observed at 25–30 °C. These biophysical parameters correlated with previously described CARs. *Tv*CAR's T_m of 55 °C indicated a higher stability compared to type III fungal CAR, *Nc*CAR, as well as other type IV CARs. Due to the tolerance of acidic pH environments and the higher stability of *Tv*CAR, it was finally applied for the reduction of DOPAC to 3-HT. 58.2 mM of 3-HT were converted in whole cell biotransformations when 60 mM of DOPAC was used within 24 h without any optimizations, which is nearly a duplication compared to the previous benchmark.

Experimental Section

General

All chemicals were obtained from Sigma-Aldrich/Merck or Roth, except otherwise noted. No further purification steps were performed. HPLC-MS grade acetonitrile was purchased from J.T.Baker/Avantor Performance Materials, Deventer, The Netherlands. Helium gas for GC-analysis was purchased from Linde Gas, Austria. For combining vector and insert fragments, the Gibson Assembly® was performed with the Gibson Assembly® HiFi 1-Step Kit by Synthetic Genomics® (Cat. Nr. GA1100-10).

Phylogenetic Analysis

30 functional CARs were analyzed (SI Table S1). The platform of phylogeny.fr provided the ready-to-use pipeline of MUSCLE for multiple alignment, PhyML for tree building, and TreeDyn for tree rendering.[41]

Expression and Purification

Gene Assembly, Cultivation and Expression

Gene sequences were equipped with an *N*-terminal His_6-tag and codon-optimized for *E. coli* K12 via the IDT optimizing tool. The gene fragments were ordered from IDT (SI Table S3). To combine the gene fragments, overlap extension PCR was conducted. PCR was carried out under the following conditions: 50 µL total volume, 200 µM of each dNTP, 0.2 µM of each primer (SI Table S2), and 2.5 U of Q5 High-Fidelity DNA polymerase. Cycling conditions were as follows: initial denaturation at 98 °C for 30 s, followed by 25 cycles of denaturation at 98 °C for 30 s, annealing at 56 °C for 30 s, extension at 72 °C for 4 min, and a final extension at 72 °C for 4 min. The plasmid pETDuet-1 with phosphopantetheinyltransferase from *E. coli* (Genbank Accession Nr. CAQ31055.1) was used for vector and gene assembly via the method by Gibson *et al.*[42] The correct construct was confirmed by automated sequencing (Microsynth) and a control digestion.

E. coli K12 MG1655 RARE (DE3) or BL21 (DE3), respectively, was transformed with the plasmid [pETDuet-1:*Ec*PPTase:HT*Xy*CAR] and colonies selected via LB/Amp. Protein expression was performed via the autoinduction protocol described by Studier.[28] After 24 h of expression at 20 °C, the cells were harvested by centrifugation and used for biotransformations or the pellet was stored at −20 °C until further use.

Expression Analysis

The culture supernatant was discarded, and the pellet was resuspended in 50 mM MES buffer, pH 7.5, containing 10 mM $MgCl_2$, 1 mM EDTA, and 1 mM DTT. The cell suspensions were transferred to pulping bottles and sonicated for 2×3 min with 80% duty cycle and output control level 8 with extensive cooling. Whole cell lysates were immediately cooled on ice and centrifuged in 50 mL tubes for 45 min at 41,533 rcf and 4 °C to pellet cell debris. The supernatant was further used for Ni-affinity chromatography. The pellet was resuspended in 2 mL of 6 M urea and incubated for 40 min at 60 °C and 700 rpm. After centrifugation for 15 min at 16,168 rcf, the concentration of the supernatant was determined via the BCA-Assay. Successful protein expression was visualized by SDS-PAGE analysis under reducing conditions. Protein samples were denatured in NuPAGE LDS Sample Buffer for 10 min at 80 °C. In general, 15 µL sample solution containing 10 µg protein for cell lysate and 5 µg for purified protein in 1X NuPAGE™ LDS Sample Buffer were loaded onto a NuPAGE Bis-Tris gels 4–12% and run at 25 mA per gel using the XCell SureLock™ Mini-Cell Electrophoresis System with a PowerEase® 500 Power Supply. Staining was performed with SimplyBlue™ SafeStain solution (LC6065, Novex®) according to the manufacturers protocol. After staining, the gel was washed with dH_2O and destained overnight in dH_2O. Bands corresponding to soluble and insoluble protein were analyzed via G:Box HR16 by Syngene (SnapGene, software by Syngene). The software Gene Tools by Syngene was used for quantification of the protein bands.

Ni-Affinity Chromatography

Cell free extracts (CFEs) were prepared by resuspending harvested cell pellets in 20 mM potassium phosphate buffer, 500 mM NaCl, pH 7.4, conatining 10 mM imidazole for purification of recombinant protein. The prepared CFE was filtered through a 0.22 µm syringe filter prior to purification. Protein purification was conducted with prepacked, ready-to-use columns on an Äkta Pure 100 with a fraction collector F950 (Unicorn 6.3 software, GE Healthcare) by applying a concentration gradient of imidazole. For buffer exchange and removal of imidazole after purification, proteins were desalted using PD-10 columns, previously equilibrated with desalting buffer (50 mM MES, pH 7.5, containing 10 mM $MgCl_2$, 1 mM EDTA, and 1 mM DTT). Aliquots of the protein solution were shock frozen in liquid nitrogen and stored at −80 °C. Protein concen-

trations were determined with a Nanodrop 2000c spectrophotometer (Thermo Scientific).

Anion-Exchange Chromatography

Frozen aliquots of Ni-affinity chromatography-purified CARs were thawed, re-buffered to 50 mM MES, pH 7.5 and loaded onto a QFF HiTrap 5 mL FF column. The anion-exchange chromatography was conducted on an Äkta Pure 100 with a fraction collector F950 (Unicorn 6.3 software, GE Healthcare) by applying a concentration gradient (0–100%) of 0.5 M NaCl. CARs eluted at approximately 27% of NaCl, which correlates to 0.135 M of NaCl. Protein concentrations were determined with a Nanodrop 2000c spectrophotometer (Thermo Scientific).

Tv2CAR Co-Expressed with Various Chaperone and Modified E. Coli Strains

E. coli strains listed in Table 2 were transfected with pETDuet-1:*Ec*PPTase:HT*Tv2*CAR (SI Figure S2). For the co-induction of the chaperone proteins, 0.5 mg mL^{-1} L-arabinose (pG-KEJ8) and/or 5 ng mL^{-1} tetracycline ([pG-KJE8], [pG-TF2]) was added before the temperature was adjusted to 20 °C.

Co-Expression of Beneficial Chaperones with Weakly Expressed TvCAR and Tv2CAR

E. coli K-12 MG1655 RARE (DE3) pETDuet-1:*Ec*PPTase:HT*Tv*CAR and *E. coli* K-12 MG1655 RARE (DE3) pETDuet-1:*Ec*PPTase:HT*Tv2*CAR were transfected with either pG-KJE8 or gG-TF2 to exploit the diminished aldehyde reduction of *E. coli* K-12 MG1655 RARE (DE3). For the co-induction of the chaperone proteins, 0.5 mg mL^{-1} L-arabinose (pG-KEJ8) and/or 5 ng mL^{-1} tetracycline (pG-KJE8, pG-TF2) was added before the temperature was adjusted to 20 °C.

Enzyme Characterization

Resting Cell Bioconversions of 1 a Determined by HPLC-UV

Resting cell bioconversions: OD_{600} values were determined and culture aliquots corresponding to 50 OD_{600} units were transferred into the wells of a 24-deep well plate. Specifically, 48.4 mg mL^{-1} of cells were used for each reaction. Cells were harvested by centrifugation for 20 min at 3,220 rcf and 4 °C. Afterwards, the supernatants were removed and pellets were carefully resuspended in 200 mM potassium phosphate buffer, pH 7.4, containing 10 mM piperonylic acid **1 a** (added from a 100 mM stock solution in KOH100 mM, pH neutral), 48 mM glucose, 24 mM sodium citrate and 4 mM $MgSO_4$. Bioconversions were carried out in 24-deep well plates covered with oxygen permeable membranes for 2 h at 28 °C and 320 rpm. The reactions were then stopped by transferring 500 µL of cell suspension into an Eppendorf tube and adding 1.5 mL of MeOH. Further, the suspensions were centrifuged for 5 min at 16,168 rcf and 22 °C. 200 µL of the supernatant were transferred into 96-well plates (V-bottom, polypropylene). At least three individual experiments were conducted. Conversions with **1 a** were determined by HPLC. For HPLC-UV analysis an Agilent Technologies 1100 Series equipped with a G1379A degasser, 1200 Series Quaternary pump G1379A, G1367A autosampler, G1330B autosampler thermostat, G1316A thermostated column compartment and a G1315B Diode Array Detector was used. The analysis of **1 a**, **1 b** and **1 c** was carried out with a Kinetex 2.6 µ Biphenyl 100 A HPLC column (Phenomenex). The mobile phases were ammonium acetate (5 mM) and 0.5% v/v acetic acid in water and acetonitrile (ACN) at a flow-rate of 0.26 mL min^{-1}. A stepwise gradient was used: 25–55% ACN (5 min), 55–70% ACN (5.0–7.2 min) 70–90% ACN (7.2–7.5 min). The compounds were detected at 254 nm (DAD) (SI Table S7).

Determination of Substrate Scope by NADPH-Depletion Monitoring

The NADPH depletion assay was used to determine initial rate activities for the reduction of short to middle-long aliphatic acids and aromatic acids. Therefore, carboxylic acids were dissolved in DMSO or KOH (each 100 mM). The assay composition was as follows: the substrate (100 mM stock solution, 5 mM end concentration) was added to MES buffer (50 mM, pH 7.5, containing 10 mM $MgCl_2$, 1 mM EDTA, and 1 mM DTT). Subsequently, 0.5 mM NADPH,1.0 mM ATP and 10 µL of CAR enzyme preparation from Ni-affinity chromatography (1.0 mg mL^{-1}) were added to a final volume of 200 µL. The depletion of NADPH was followed on a Synergy Mx Plate reader (BioTek) at 340 nm and 28 °C for 10 min. Blank reactions (ATP omitted) were carried out in parallel and each reaction was carried out in triplicates.

In Vitro Activity Assay for Determination of pH Optima of TvCAR

2 mM Octanoic acid (**7 a**) in DMSO (0.1 M) were added to 100 mM MES buffer, pH 7.5, containing 10 mM $MgCl_2$, 1 mM EDTA, and 1 mM DTT. 90 µL of enzyme preparation from Ni-affinity chromatography (1 mg mL^{-1}) were added to the reaction mix. 1.2 mM ATP and NADPH were added to start the reaction. The *in vitro* activity assay was performed in a total volume of 600 µL in Eppendorf reaction tubes at 28 °C and 700 rpm for 3 h in a Thermomixer comfort (Eppendorf). To stop the reaction, the solution was acidified to pH 2.0 with 3 M HCl. Extraction of fatty acid, aldehyde and alcohol was achieved with two times 400 µL of ethyl acetate, including 0.01% tetradecane as internal standard (IS). Afterwards, the mixture was vortexed for 10 min and centrifuged for 15 min at 16,168 rcf and 4 °C. The organic phase containing the extracted fatty acid, aldehyde, alcohol and IS was transferred to a fresh Eppendorf tube and dried with Na_2SO_4 (approximately 10% w/v). 190 µL of the mixture were transferred into glass vials for GC analysis. For the analysis of fatty acid concentration, at least technical triplicates were carried out. Quantitation was performed based on linear interpolation of calibration curves with concentrations of standards from 0.156 mM to 30 mM. Analysis of **7 a**–**c** was carried out on an Optima 1 MS column (100% dimethylpolysiloxane; 30 m, 0.25 mm in diameter and 0.25 µm film thickness) on a Shimadzu GCMS-QP2010 SE equipped with a mass selective detector. Sample aliquots of 1 µL were injected in split mode (split ratio 6.5:1) at 240 °C injector temperature and 320 °C detector temperature with helium as carrier gas. The temperature program was as follows: 70 °C for 5 min and a ramp to 300 °C at 15 °C min^{-1}. The total run time was 24.26 min (SI Table S5). The mass selective detector was operated in a mass range of 30–500 m/z. GC-MS results were evaluated with the GC-MS Data Analysis software LabSolution by Shimadzu.

Determination of Optimal pH of Tv2CAR and DsCAR

CARs were investigated in the pH range of 5.5–9.0 in intervals of 0.5 pH units. All buffers (100 mM, supplemented with 10 $MgCl_2$), were adjusted to the desired pH value with either NaOH or HCl at 25 °C. Specifically, MES-NaOH pH 6.0–7.5, potassium phosphate pH 6.0–7.5, bicine-NaOH pH 7.0–8.0 and Tris-HCl pH 7.5–9.0 were applied. All other parameters were applied as described in *in vitro* activity

assay. Activity was calculated relative to the maximum rate at 100%.

Determination of Optimal Temperature

HEPES-NaOH buffer (100 mM), pH 7.5, containing 10 mM $MgCl_2$, 1 mM EDTA and 1 mM DTT was prepared at temperatures ranging from 25 to 50 °C. The enzyme preparations were preincubated for 1 h at each temperature. Residual activity was determined as described in *in vitro* activity assay. Activity was calculated relative to the maximum rate at 100%.

Determination of pI of TvCAR

Ni-affinity chromatography purified samples, in 10 mM MES buffer, were mixed with SERVALYT™ carrier ampholytes and separated on a Rotofor® Cell (Bio-Rad). The pI was determined through determination of the pH of each protein fraction and loading each protein fraction onto SDS-PAGE.

Thermostability Determination via Thermal Shift Assays

The temperature stability of CARs was investigated after two step purification by Ni-affinity chromatography and anion exchange chromatography by monitoring the fluorescence of a solvatochromic dye (ThermoFluor®)[35,43] 20 mg mL^{-1} of each CAR was added to SYPRO Orange (1:200 dilution) and 100 mM buffer pH 4.6–9.0. Sodium acetate pH 4.6–5.5, sodium citrate pH 5.5–6.5, MES-NaOH pH 5.5–6.5, potassium phosphate pH 6.0–8.0, HEPES-NaOH 7.5–8.0, bicine-NaOH pH 7.0–9.0 and Tris-HCl pH 8.0–9.0 were used. The samples were measured in triplicates with CFX96 touch detection system (Bio-Rad). The temperature profile started from 20 °C to 95 °C in a gradient of 1 °C min^{-1}. The fluorescence emission of the dye was determined with HEX fluorescence emission filter to monitor unfolding of the protein. The T_m is defined as the temperature at the inflection point of the corresponding melting curve.

Improved Bioconversion of DOPAC to 3-hydroxytyrosol by *Tv*CAR

Resting Cell Bioconversions of DOPAC (3 a) Determined by HPLC-MS

Resting cell bioconversions: OD_{600} values were determined and culture aliquots corresponding to 50 OD units were transferred into Pyrex™ tubes. Cell pellets were harvested by centrifugation for 20 min at 3,220 rcf and 4 °C. Afterwards, the supernatants were removed and pellets were carefully resuspended in 1.5 mL of 200 mM MES buffer, pH 6.0, containing 10–60 mM DOPAC (**3 a**), 10 mM $MgCl_2$, 20 mM glucose, 48 mM sodium citrate and 8 mM $MgSO_4$. Bioconversions were carried out in glass cultivating tubes up to 24 h at 28 °C in a tissue rotator. The suspensions were transferred to Eppendorf tubes and centrifuged for 40 min at 16,168 rcf. 200 µL of the supernatant were transferred into 96-well plates (V-bottom, polypropylene). At least three individual experiments, i.e. technical triplicates, were conducted.

Conversions with **3 a** were determined by HPLC-MS. For HPLC-MS measurements, an Agilent Technologies 1200 Series equipped with G1379B degasser, G1312B binary pump SL, G1367C HiP-ALS SL autosampler, a G1314C VWD SL UV detector, G1316B TCC SL column oven, and a G1956B mass-selective detector (MSD) were used. Samples were filtered through an AcroPrep 96 Filter Plate (Pall Life Science) with 0.2 mm polypropylene membrane prior to analysis. 3,4-Dihydroxyphenylacetic acid (**3 a**), 3,4-dihydroxyphenylacetaldehyde (**3 b**), and 3-HT (**3 c**) were separated on a Chromolith Performance RP-18 endcapped 100–4.6 column (Merck) at 30 °C by using a 95% aqueous eluent (0.1% formic acid) and 5% ACN at a flow of 0.8 mL min^{-1} (SI Table S8).

Acknowledgements

Giuseppe Fiume, Daniel Schwendenwein and Sandy Schmidt are greatly acknowledged for technical assistance. The authors thank Fredi Brühlmann and Andreas Taglieber for valuable discussions as well as Kristala L. J. Prather for generously providing Escherichia coli *K-12 MG1655 RARE (DE3). The Austrian Research Promotion Agency FFG (P 860262) and Firmenich SA are kindly acknowledged for the financial support. This research has also been supported by the Austrian BMWFW, BMVIT, SFG, Standort Tirol, Government of Lower Austria and ZIT through Austrian FFG-COMET-Funding Program.*

Conflict of Interest

The authors declare no conflict of interest.

Keywords: carboxylate reductase (CAR) · *in vivo* biotransformation · carboxylic acid · reduction · antioxidant

[1] Y. H. P. Zhang, *Biotechnol. Adv.* **2015**, *33*, 1467–1483.
[2] U. Hanefeld, R. A. Sheldon, I. Arends, *Electrochemistry*, **2007**, *2*, 1–20.
[3] R. Cernansky, *Nature* **2015**, *519*, 379–380.
[4] J. D. Keasling, *Science* **2003**, *330*, 1355–1358.
[5] J. D. Keasling, *Metab. Eng.* **2012**, *14*, 189–195.
[6] D. Gahloth, M. S. Dunstan, D. Quaglia, E. Klumbys, M. P. Lockhart-Cairns, A. M. Hill, S. R. Derrington, N. S. Scrutton, N. J. Turner, D. Leys, *Nat. Chem. Biol.* **2017**, *13*, 975–981.
[7] M. Ahsan, S. Sung, H. Jeon, M. Patil, T. Chung, H. Yun, *Catalysts* **2017**, *8*, 4.
[8] M. K. Akhtar, N. J. Turner, P. R. Jones, *Proc. Natl. Acad. Sci. USA* **2013**, *110*, 87–92.
[9] Z. Hu, *US 2010/0105963 A1* **2010**, 1–46.
[10] L. Kramer, E. D. Hankore, Y. Liu, K. Liu, E. Jimenez, J. Guo, W. Niu, *ChemBioChem* **2018**, *19*, 1452–1460.
[11] G. Qu, J. Guo, D. Yang, Z. Sun, *Green Chem.* **2018**, *20*, 777–792.
[12] H. Stolterfoht, D. Schwendenwein, C. W. Sensen, F. Rudroff, M. Winkler, *J. Biotechnol.* **2017**, *257*, 222–232.
[13] G. G. Gross, *Eur. J. Biochem.* **1972**, *31*, 585–592.
[14] D. Schwendenwein, G. Fiume, H. Weber, F. Rudroff, M. Winkler, *Adv. Synth. Catal.* **2016**, *358*, 3414–3421.
[15] P. Venkitasubramanian, L. Daniels, J. P. N. Rosazza, *J. Biol. Chem.* **2007**, *282*, 478–485.
[16] H. Stolterfoht, G. Steinkellner, D. Schwendenwein, T. Pavkov-Keller, K. Gruber, M. Winkler, *Front. Microbiol.* **2018**, *9*, 250.
[17] M. Wang, M. Beissner, H. Zhao, *Chem. Biol.* **2014**, *21*, 257–63.
[18] C. Li, Y. Matsuda, H. Gao, D. Hu, X. S. Yao, I. Abe, *ChemBioChem*, **2016**, *17*, 904–907.
[19] M. Winkler, C. K. Winkler, *Monatshefte für Chemie - Chem. Mon.* **2016**, *147*, 575–578.
[20] M. Wang, H. Zhao, *ACS Catal.* **2014**, *4*, 1219–1225.
[21] T. Li, J. P. N. Rosazza, *J. Bacteriol.* **1997**, *179*, 3482–3487.
[22] A. He, T. Li, L. Daniels, I. Fotheringham, J. P. N. Rosazza, *Appl. Environ. Microbiol.* **2004**, *70*, 1874–1881.
[23] Y. Duan, P. Yao, X. Chen, X. Liu, R. Zhang, J. Feng, Q. Wu, D. Zhu, *J. Mol. Catal. B* **2015**, *115*, 1–7.

[24] W. Finnigan, A. Thomas, H. Cromar, B. Gough, R. Snajdrova, J. P. Adams, J. A. Littlechild, N. J. Harmer, *ChemCatChem* **2017**, *9*, 1005–1017.
[25] A. M. Kunjapur, Y. Tarasova, K. L. J. Prather, *J. Am. Chem. Soc.* **2014**, *136*, 11644–11654.
[26] H. P. Sørensen, K. K. Mortensen, *Microb. Cell Fact.* **2005**, *4*, 1–8.
[27] A. K. Hess, P. Saffert, K. Liebeton, Z. Ignatova, *PLoS One* **2015**, *10*, 1–14.
[28] F. W. Studier, *Protein Expression Purif.* **2005**, *41*, 207–234.
[29] C. C. R. Carvalho, R. M. M. Fonseca, *Dyn. Biochem. Process Biotechnol. Mol. Biol.* **2007**, *1*, 32–39.
[30] B. Lin, Y. Tao, *Microb. Cell Fact.* **2017**, *16*, 1–12.
[31] K. Nishihara, M. Kanemori, H. Yanagi, T. Yura, *Appl. Environ. Microbiol.***2000**, *66*, 884–889.
[32] K. Nishihara, M. Kanemori, M. Kitagawa, H. Yanagi, T. Yura, *Appl. Environ. Microbiol.* **1998**, *64*, 1694–1699.
[33] O. Kandror, M. Sherman, R. Moerschell, A. L. Goldberg, *J. Biol. Chem.* **1997**, *272*, 1730–1734.
[34] K. Talley, E. Alexov, *Proteins* **2010**, *78*, 2699–2706.
[35] U. B. Ericsson, B. M. Hallberg, G. T. DeTitta, N. Dekker, P. Nordlund, *Anal. Biochem.* **2006**, *357*, 289–298.
[36] Y. Achmon, A. Fishman, *Appl. Microbiol. Biotechnol.* **2014**, *99*, 1119–1130.
[37] E. B. Bali, V. Ergin, L. Rackova, O. Bayraktar, N. Küçükboyaci, Ç. Karasu, *Planta Med.* **2014**, *80*, 984–992.
[38] S. Burattini, S. Salucci, V. Baldassarri, A. Accorsi, E. Piatti, A. Madrona, J. L. Espartero, M. Candiracci, G. Zappia, E. Falcieri, *Food Chem. Toxicol.* **2013**, *55*, 248–256.
[39] K. Napora-Wijata, Ch. Rijksen, K. Robinson, A. V. Osorio Lozada, M. Winkler, *WO 2014/090923 Al* **2014**, 1–65.
[40] K. Napora-Wijata, K. Robins, A. Osorio-Lozada, M. Winkler, *ChemCatChem* **2014**, *6*, 1089–1095.
[41] A. Dereeper, V. Guignon, G. Blanc, S. Audic, S. Buffet, F. Chevenet, J.-F. Dufayard, S. Guindon, V. Lefort, M. Lescot, J.-M. Claverie, O. Gascuel, *Nucleic Acids Res.* **2008**, *36*, 465–469.
[42] D. G. Gibson, L. Young, R.-Y. Chuang, J. C. Venter, C. A. Hutchison, H. O. Smith, *Nat. Methods* **2009**, *6*, 343–5.
[43] J. J. Lavinder, S. B. Hari, B. J. Sullivan, T. J. Magliery, *J. Am. Chem. Soc.* **2009**, *131*, 3794–3795.

Manuscript received: February 25, 2019
Revised manuscript received: March 18, 2019
Version of record online: April 9, 2019